



Experiments and simulations on low-temperature waste heat harvesting system by thermoelectric power generators

Cheng-Ting Hsu^a, Gia-Yeh Huang^b, Hsu-Shen Chu^c, Ben Yu^d, Da-Jeng Yao^{a,b,*}

^a Institute of NanoEngineering and MicroSystems, National Tsing Hua University, Hsinchu 30013, Taiwan, ROC

^b Department of Power Mechanical Engineering, National Tsing Hua University, Hsinchu 30013, Taiwan, ROC

^c Material and Chemical Research Laboratories, Industrial Technology Research Institute, Hsinchu, Taiwan, ROC

^d Wise Life Technology Co., Ltd., Hsinchu, Taiwan, ROC

ARTICLE INFO

Article history:

Received 29 July 2010

Received in revised form 30 September 2010

Accepted 6 October 2010

Available online 30 October 2010

Keywords:

Waste heat

Recovery

Thermoelectric

Generator

Exhaust pipe

Simulation

ABSTRACT

In this case study, a system to recover waste heat comprised 24 thermoelectric generators (TEG) to convert heat from the exhaust pipe of an automobile to electrical energy has been constructed. Simulations and experiments for the thermoelectric module in this system are undertaken to assess the feasibility of these applications. A slopping block is designed on the basis of simulation results to uniform the interior thermal field that improves the performance of TEG modules. Besides simulations, the system is designed and assembled. Measurements followed the connection of the system to the middle of an exhaust pipe. Open circuit voltage and maximum power output of the system are characterized as a function of temperature difference. Through these simulations and experiments, the power generated with a commercial TEG module is presented. Overview this case study and our previous work, the results establish the fundamental development of low-temperature waste heat thermoelectric generator system that enhances the TEG efficiency for vehicles.

© 2010 Elsevier Ltd. All rights reserved.

1. Introduction

Because of the increasing emphasis on environmental protection, applications of thermoelectric technology are extensively studied. Thermoelectric generator (TEG) may offer thermoelectric energy conversion in a simple and reliable way. In addition, a TEG module has many advantages such as no moving parts, quite and being environmental friendly. Due to these merits, the use of TEG to harvest waste heat has been comprehensively discussed in many industrial fields. Over the last 30 years, there has been growing interest in applying this thermoelectric technology to improve the efficiency of waste heat recovery, using the various heat sources such as geothermal energy, power plants, automobiles and other industrial heat-generating process [1–12].

However, the primary challenge of the thermoelectric power generation is its relatively low heat-to-electricity conversion efficiency. Researching groups world wide are now making efforts to improve the intrinsic conversion efficiency of the thermoelectric materials, such as BiTe, ZnBe, CeFeSb, SiGe and even new nanocrystalline or nanowire thermoelectric materials [13–15]. Somehow,

the scaling of nanomaterials is quite difficult to apply it in practice in our daily life, so it is still in its developing stage. In the case of waste heat recovery power generation, there are many conceptual designs in automobiles. Most of them used BiTe-based bulk thermoelectric material because it is made commercially available. Hi-Z Technology [16], tried to discover and to improve the efficiency of thermoelectric modules. HZ-14 modules are based on Bi₂Te₃, of theoretical and experimental efficiency to about 5% [4]; the goal of Hi-Z for a practical device is an efficiency about 20%. Imaging that if the replacement of the 1 kW, TEG unit with that efficiency would attain fuel consumption decreased between 12% and 30%. For the applications of thermoelectric technology in automobiles, Hsiao and Chang [17] have constructed a mathematic model to predict the performance of a TEG module attached to the waste heat recovery system. The results show that the TEG module presents better performance on the exhaust pipe than on the radiator. Recently, Thacher et al. [18] investigated the feasibility of waste heat recovery from exhaust in a light truck by series connecting 16 BiTe-based TEG modules, which showed good performance at high speeds. After that, Niu [19] connected 56 BiTe-based TEG modules in series to show the promising potential of using TEG for low-temperature waste heat recovery. Which also shows good conversion efficiency ($\eta \sim 4.44\%$). In order to enhance the performance, Gou [20] proposed many suggestions to obtain better performance, such as increasing the waste heat temperature

* Corresponding author at: Institute of NanoEngineering and MicroSystems, National Tsing Hua University, Hsinchu 30013, Taiwan, ROC. Tel.: +886 3 5715131x42850; fax: +886 3 5745454.

E-mail address: djyao@mx.nthu.edu.tw (D.-J. Yao).

and TEG modules in series, expanding heat sink surface area in a proper range and enhancing cold-side heat transfer capacity.

In the previous study, we constructed a thermal resistor network to analyze one pair of thermoelectric legs which helps to predict power output more precisely. Furthermore, a simulation model also constructed to investigate the thermal field distributions and system power output prediction, these results are verified with experiments [21,22]. In this study, a further analysis of previous work is considered which pertinent thermoelectric equations are presented, and the simulation results were used to choose a suitable heat sink [22]. Transforming the energy of waste heat into electricity, especially for vehicles and motorcycles, is the specific issue of this research. A system to recover waste heat has been designed, simulated and fabricated to achieve the objective of recovered energy, as explained in the following sections.

2. Experimental setup

This waste heat recovery system is designed for exhaust pipe of automobiles. TEG modules (TMH400302055, Wise Life Technology, Taiwan) are connected electrically in series but thermally in parallel, and these modules are arranged on the both surfaces of aluminum heat exchanger through which the exhaust gas is passed. Fig. 1 shows the schematic diagram of the experimental waste heat recovery system. Some measuring instruments are equipped to construct this experimental setup. A power supply (HP 6032A system power supply) is used to drive these fans to cool the heat sinks. T-type thermal couples are embedded in hot and cold sides of TEG modules to record temperature while measuring. A high power electrical resistor array is connected in series to the system which is used to capture the matching load for the optimized power output. The ammeter and the voltmeter are connected to measure the current in the circuit and voltage cross the external load resistor respectively.

3. Simulation analysis

3.1. System architecture

Continuation of the first-generation waste heat recovery system of previous studies [22], a second-generation one is constructed which increases the dimension of the original one, as shown in Fig. 2. The size is enlarged from 27 to 54 cm in length, 17 to 23.6 cm in width and 23.6 to 29.6 cm in height respectively. Besides, the number of TEG modules is increased from 8 to 24.

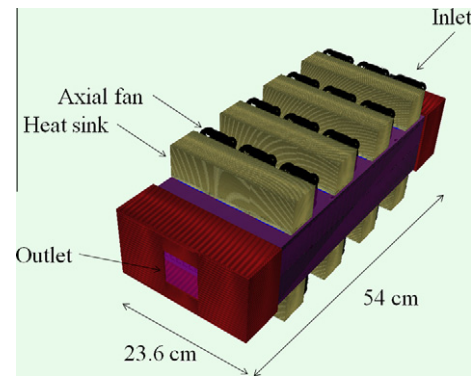


Fig. 2. Prototype of the 2nd generation waste heat recovery system.

Table 1

Boundary conditions in these series simulations.

Ambient temperature (K)	300
Ambient heat transfer coefficient ($\text{W m}^{-2} \text{K}^{-1}$)	10
Internal flow speed (m s^{-1})	12
Internal flow temperature (K)	573
Dimension of fan (mm^3)	$60 \times 60 \times 25$
Flow rate of fan ($\text{m}^3 \text{s}^{-1}$)	1.04×10^{-2}
Material of heat sink	Copper
Dimension of heat sink (mm^3)	$56.5 \times 76 \times 60$ (h)
Number of fins (heat sink)	44
Fin thickness of heat sink (mm)	0.4
Base thickness of heat sink	5
Material of heat exchanger	Aluminum
Dimension of heat exchanger (mm^3)	$540 \times 236 \times 60$ (h)
Fin thickness of heat exchanger (mm)	2.5
Base thickness of heat exchanger (mm)	8

Table 1 shows the boundary conditions and dimensions of each element in these series simulations. The system design of these thermal management solutions was supported by using commercially available Computational Fluid Dynamics (CFD) software, FloTherm. Limitations of the selected TE module restrict the allowable hot-side working fluid temperatures are generally less than 573 K. Therefore this specific temperature of 573 K is selected as the exhaust temperature in simulations. For the external flow (of cooling air), the axial fan (Minebea–Matsushita 2410ML-04 W-B86) had a flow speed $1.04 \times 10^{-2} \text{ m}^3 \text{s}^{-1}$ (according to the vendor's data sheet). Consequently, the fan flow of this speed is considered in simulations while the ambient temperature is set to be 300 K.

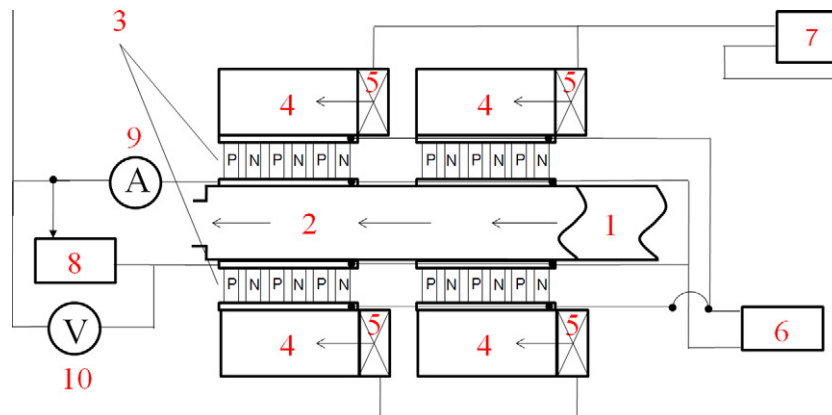


Fig. 1. Schematic diagram of the experimental waste heat recovery system. 1: Exhaust pipe of automobiles. 2: Heat exchanger for passing exhaust gas. 3: TEG modules. 4: Heat sinks. 5: Axial fans. 6: Thermal couples. 7: Power supply. 8: High power electrical resistor array. 9: Ammeter. 10: Voltmeter.

3.2. Thermal field distribution

It is worth noting that before the system is assembled, simulations would help to enhance the further design. For this specific case, the diameter of vehicle exhaust pipe is 65 mm but the heat exchanger of this waste heat recovery system is designed 236 mm in width. There is a sudden expansion as exhaust flow through the exhaust pipe into the system, which leads to an uneven thermal distribution inside the heat exchanger. That is, most of the heat sources are concentrated in the middle part of heat exchanger while only a small part of heat pass through the both sides, as shown in Fig. 3a. It will seriously influence the overall performance of TEG modules. Accordingly, TEG modules attached to the both sides perform much worse than that attached on the central row. To improve this phenomenon, slopping block is introduced in the inlet of sudden expansion, as shown in Fig. 3b or Fig. 4c. The slopping block separates the heat source into three

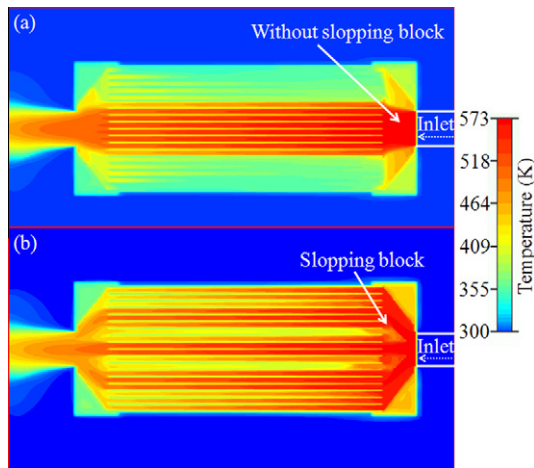


Fig. 3. Schematic diagram of steady state thermal field distribution: (a) and (b) investigate aluminum heat exchanger without and with slopping block in the inlet sudden expansion respectively.

parts which makes thermal distribution more uniform, and the performance of TEG modules on both sides is expected to get improved.

During simulations of Fig. 3a and b, the ambient temperature is assigned for 300 K. However, heat may accumulate in the system and the ambient temperature would increase for a short period of time. Regardless of this transient phenomenon, Fig. 3 is captured in steady state operational results.

4. Measurement

4.1. System setup

To estimate the output performance of this case study, the waste heat recovery system is setup, as shown in Fig. 4. Fig. 4a illustrates the TEG module with 199 pairs of TE legs employed in this application. The geometric features and transport properties of a pair of TE leg are listed in Table 2 [22]. Fig. 4b and c shows the photographs of outlet and inlet cover respectively. Notably, the slopping block is installed in the inlet due to the simulation result. Fig. 4d shows the photograph of a 19-fin structured aluminum heat sink which operates as a heat exchanger to extract waste heat energy. Fig. 4e shows the photograph of semifinished system. The copper heat sink and the axial fan (Minebea–Matsushita 2410ML-04 W-B86) upon the TEG module should decrease the temperature at the cold side of the TEG to generate a larger temperature difference. The bakelite frame which is used to fix and define the location of TEG modules are also presented in Fig. 4e. This bakelite frame is considered as an effectively thermally isolated material to prevent loss of thermal energy. Fig. 4f shows the photograph of waste heat recovery system. Two 19-fin structured aluminum heat sinks are assembled oppositely as a heat exchanger for waste gases passing through. The fin structures are made up heat exchanging more effectively than that without fin structures which is discussed in previous study. There are 24 TEG modules sandwiched between heat sinks and the heat exchanger in this system. Other detailed dimensions of the each component are listed in Table 1. In order to reduce thermal contact resistance, a thermal interface material, thermal grease, was smeared uniformly on the both side of TEG module.

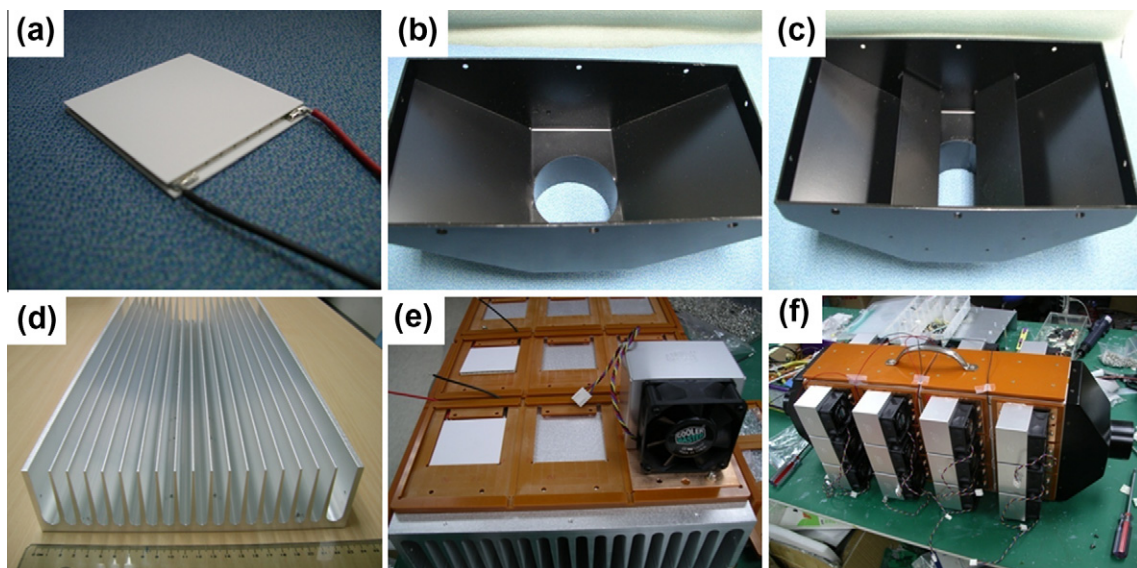


Fig. 4. Schematic diagram of the waste heat recovery system: (a) TEG module. (b) The outlet cover. (c) Sudden expansion inlet with slopping block. (d) 19-fin structured aluminum heat sink. (e) and (f) are semifinished and completely finished system.

Table 2

Geometric features and transport properties of a pair of TE leg.

Parameter @ 300 K	N-type element	P-type element	Copper	Ceramic	Solder	Thermal grease
Seebeck coefficient ($V K^{-1}$)	-2.12×10^{-4}	2.15×10^{-4}	N/A	N/A	N/A	N/A
Resistivity (Ωm)	1.04×10^{-5}	1.04×10^{-5}	3.2×10^{-8}	1×10^{12}	12.1×10^{-8}	N/A
Thermal conductivity ($W m^{-1} K^{-1}$)	1.456	1.373	385	22	50	3
$Z (K^{-1})$	0.209×10^{-3}	3.23×10^{-3}	N/A	N/A	N/A	N/A
Thermal resistivity ($K W^{-1}$)	109.89	116.79	0.1443	3.207	0.25	0.74
Contact area (m^2)	4×10^{-6}	4×10^{-6}	9×10^{-6}	9×10^{-6}	4×10^{-6}	9×10^{-6}
Thickness (m)	6.4×10^{-4}	6.4×10^{-4}	5×10^{-4}	6.35×10^{-4}	5×10^{-5}	2×10^{-5}

4.2. A single TEG module testing

Before the system performance testing, a performance prediction should be achieved by means of testing a single TEG module. A TEG measurement system was used to measure the performance of a TEG module. A sandwiched structure (from top to bottom) of heater/copper plate/TEG module/copper plate/liquid cooling system was introduced to measure a single TEG module. Thus the TEG module was clamped between two copper plates. Two thermocouples were inserted into these two copper plates respectively to measure the temperature difference between the hot and cold sides of a TEG module. The coolant (water) was supplied from a water-circulating chiller to maintain a cold-side temperature (T_c). For a temperature difference ΔT applied to a TEG module, the internal resistance could be calculated by measuring open circuit voltage, V_{oc} . In this circuit, the matching load point occurs when $1/2 V_{oc}$ is captured by the data acquisition system. The power gen-

erated with the TEG is estimated by the value of $1/2 V_{oc}$ and the current in the circuit. For this single TEG module testing, Fig. 5a and b shows the measuring results of V_{oc} and power output for different ΔT respectively. While processing this experiment, a pressure load of 12 kg W (or 0.423 kg/cm^2) was applied to clamp the TEG module to reduce the thermal contact effect.

4.3. System performance testing

In order to find a suitable heat source, the system is connected to the middle of an exhaust pipe of an automobile (Chrysler Neon 2000 cm^3). Experimental setup is described in Fig. 1. Fig. 6 shows the measured curves of output voltage versus current and indicated in straight lines for different ΔT . Where ΔT (multi-point average) refers temperature difference between both sides of TEG

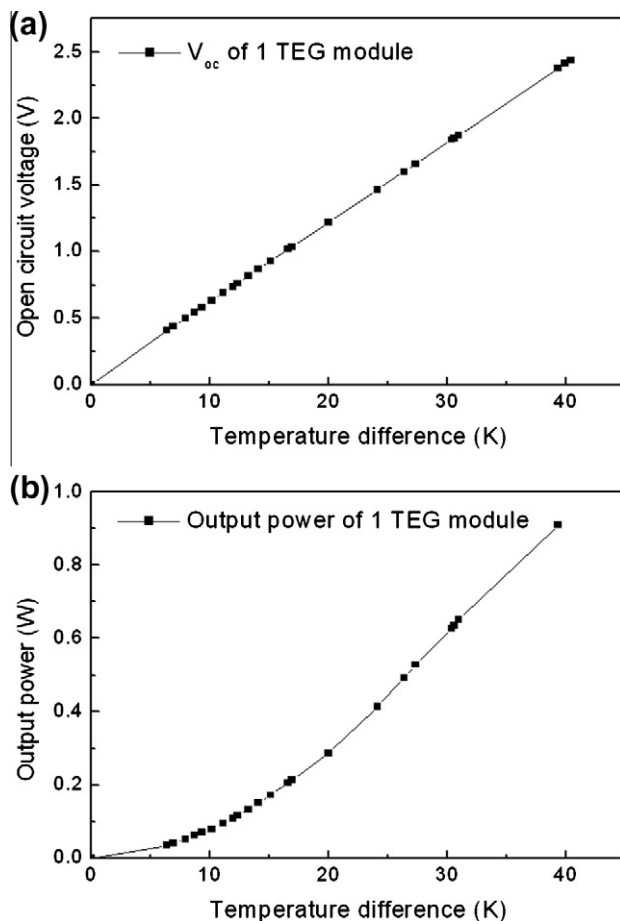


Fig. 5. Measuring results of a single TEG module: (a) Curves of open circuit voltage for different ΔT . (b) Output power for different ΔT .

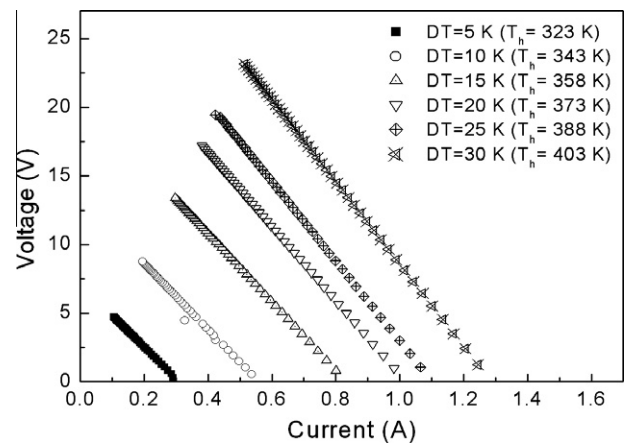


Fig. 6. Curves of output voltage-current for different ΔT .

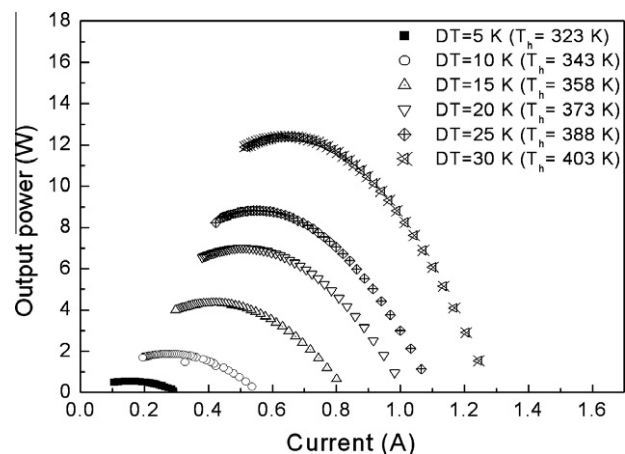


Fig. 7. Curves of output power-current for different ΔT .

modules, and T_h (multi-point average) refers to surface temperature of aluminum heat exchanger.

Fig. 7 shows the curves of output power versus current for different ΔT , which shows a maximum electrical power output for every value of ΔT at matching load condition. These values are used to create Figs. 8–10.

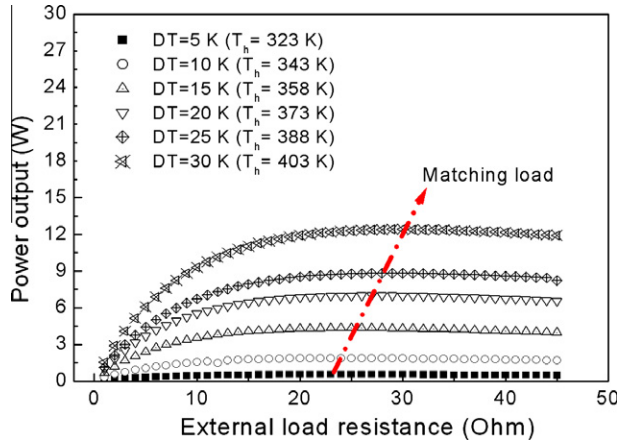


Fig. 8. Curves of external electrical resistance–power for different ΔT .

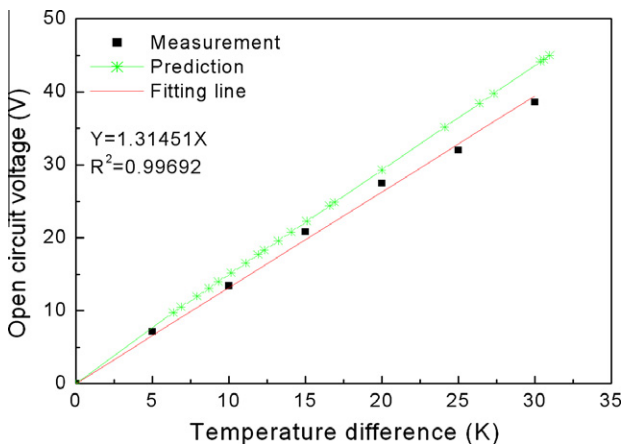


Fig. 9. Open circuit voltage for different ΔT .

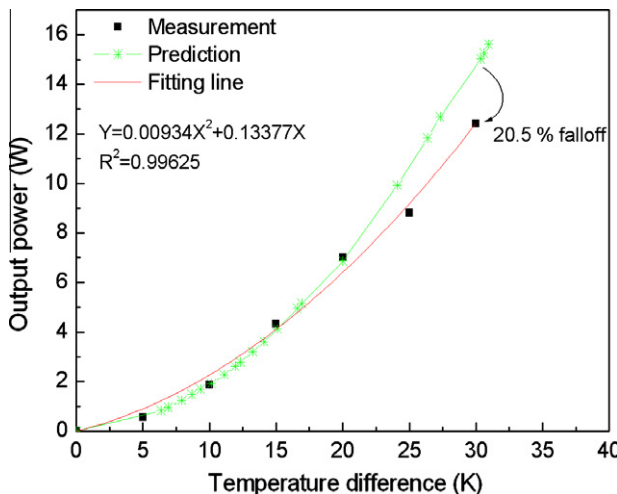


Fig. 10. Power generated for different ΔT .

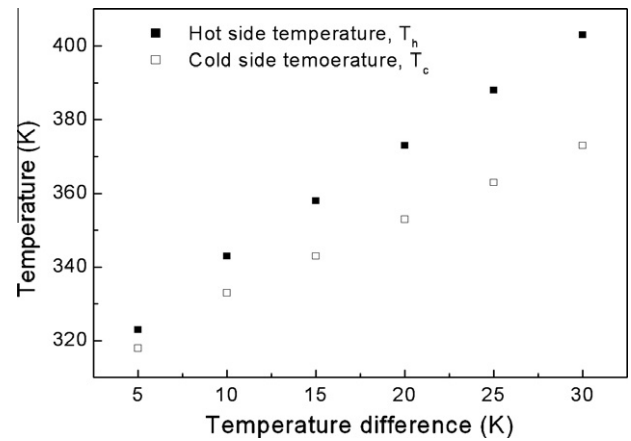


Fig. 11. Average hot and cold-side temperature of TEG modules (T_h , T_c) related to the different ΔT .

Measurements of the impedance matching for different ΔT of the system have been recorded in varying the external load from 1 to 45 Ω , shown in Fig. 8. The external load, a high power electrical resistor array of 1–45 Ω , connected in series with the system. The maximal power output is in a range of external load 23–30 Ω as ΔT increased from 5 to 30 K. Matching load is obtained to be increased with increasing ΔT (or T_h), this is due to the temperature dependence of the material properties (electrical resistance) of TE element.

Fig. 9 shows the generated open circuit voltage increases almost linearly based on a function of ΔT between both sides of TEG module. Approximately, each addition of 5 K to ΔT will result in about 6.4 V addition of open circuit voltage. Fig. 10 shows the results of the variation in the generated power relative to the ΔT . An electrical power of 12.41 W was generated with a current of 0.64 A when ΔT is 30 K.

4.4. Discussion

In this experimental condition, it is very difficult to maintain a fixed cold-side temperature (T_c). That is, with the increasing waste heat energy from the engine by boosting engine rate, the values of ΔT , T_h and T_c all get increased in this specific case study. Fig. 11 illustrates the multi-point averaged hot and cold-side temperature of TEG modules (T_h , T_c) related to the different ΔT . The results show that both T_h and T_c of TEG modules increase with the ΔT . There is a temperature difference up to 30 K when T_h reaches 403 K, resulting in a performance of 38.6 V(open circuit voltage)/12.41 W.

Table 3 shows the comparison of the performance between previous work [22] and this case study. While the engine rate fixed at 3500 RPM, there is a temperature difference of 88.3 K when T_h reaches 432 K, which is resulting in a performance of 45.26 V_{oc}/44.13 W in the 1st system. On the other hand, there is a tempera-

Table 3

Comparison of the performance between previous work and this case study.

	1st Generation	2nd Generation
Engine rate at 3.5 kRPM		
Dimensions (cm ³)	27 × 17 × 23.6 (h)	54 × 23.6 × 29.6 (h)
Number of TEGs	8	24
V _{oc} (V)	45.26	38.6
I (A)	1.95	0.64
ΔT (K)	88.3	30
Maximum power (W)	44.13	12.41
Q _{in} (kW)	2.04	3.62
Efficiency (%)	2.1	0.3

ture difference of 30 K when T_h reaches 403 K, which is resulting in a performance of $38.6V_{oc}/12.41$ W in the 2nd system at the same engine rate of 3500 RPM. The system power output of 1st generation seems much better than 2nd one. To discuss this phenomenon, system simulation of CFD software, FloTherm is used to explore the reasons. According to parameters described in Table 1, there is about 17 kW of waste heat energy passing through the inlet of this waste heat recovery system, where the heat energy is defined as

$$Q = C_p \dot{m} T \quad (1)$$

in which Q is the heat energy, C_p is specific heat of air (here, 1005 J/kg K), \dot{m} is the mass flow rate and T is the temperature based on 273 K. Furthermore, the mass flow rate is defined as

$$\dot{m} = \rho AV \quad (2)$$

in which ρ is the density of air (here, 1.1614 kg/m³), A is the cross sectional area of exhaust pipe and V is the flow velocity. As a result of simulation, when 17 kW of heat energy pass into the 1st and 2nd system respectively, there is about 3.8 kW of heat energy kept in the 1st system while 5.8 kW of heat energy is kept in the 2nd system. The remainder is passed to the ambient in the form of waste heat. The 2nd system keeps more heat energy because its interior space is much larger than the 1st one. However, there are 24 TEG modules attached on the 2nd system while 8 TEG modules are attached on the 1st one. In contrast with the two systems, each TEG module in the 2nd system absorbed less heat energy than the 1st one by >50%. Referring to the simulation results, the amount of heat energy (Q_{in}) which is transferred from the heat exchanger to the whole TEG modules is 2.04 kW in the 1st system and 3.62 kW in the 2nd one. For the two values of Q_{in} divided by the number of TEG modules in each system, the 2nd system does not perform well because the insufficient Q_{in} through the TEGs. Therefore, the average temperature difference ($\Delta T = 88.3$ K) of the 1st system is much larger than that of the 2nd one ($\Delta T = 30$ K) when the same input heat energy (~ 17 kW) is applied.

Referring to Fig. 9, the generated open circuit voltage (V_{oc}), with 24 TEG modules as a linear function of the temperature difference between their hot and cold side (ΔT), can be fitted by

$$V_{oc} = 1.31451\Delta T \quad (3)$$

and the generated maximum power (P_{max}) with 24 TEG modules as a second-ordered function of ΔT can be fitted by

$$P_{max} = 0.00934\Delta T^2 + 0.13377\Delta T \quad (4)$$

In order to modify this system, the fitting lines of Eqs. (3) and (4) are investigated in Figs. 9 and 10 respectively. R-square represents the explanation ability of a regression model. The values of R-square in Figs. 9 and 10 are 0.99692 and 0.99625 respectively which imply the accuracy of the fitting lines that explain our measurement results are more than 99%. On the basis of the above discussion, increasing waste heat temperature is advantageous to promote system performance. A notably analysis result can be obtained that there would be $131.45V_{oc}/106.77$ W with an appropriate heat source which can boost the ΔT up to 100 K according to Eqs. (3) and (4).

Moreover, thermal contact effect and heat loss problem that occurred during the assembling process caused the falloff of the generated power output at the TEG modules. The values of the falloff are about 20.5% between the predicted curve and measured result at $\Delta T = 30$ K, as shown in Fig. 10. At low temperatures, there is relatively good agreement between the predicted performance and the measurements. However, the deviation of the prediction extends largely with increasing ΔT as $\Delta T > 25$ K (or $T_h > 388$ K). In addition to thermal contact effect and heat loss problem, this specific deviation as $\Delta T > 25$ K (or $T_h > 388$ K) might be caused by un-

even thermal field distribution as described in Fig. 3. When waste heat temperature increased by boosting engine rate, the phenomenon of uneven thermal field distribution dominates which leads to uneven ΔT between each TEG modules. One TEG module out of the system with unexpectedly smaller ΔT will influence the overall performance of the entire TEG network since these TEG modules are all connected in series electrically. Thence the uneven thermal field distribution that causes the deviation between the predictions and measurements extends largely with increasing ΔT (or T_h) is assumed in this case. Supplement with the predicted curves in Figs. 9 and 10 they are proportional to expand 24 times of the results in Fig. 5a and b.

5. Conclusion

The subjective of this topic makes efforts in simulating and testing the performance of Bi₂Te₃-based TEG module. Power outputs with the system are also determined for different ΔT . Through the simulation result, the design of slopping block makes thermal distribution more uniform than that without the slopping block. Thus the performance of TEG modules on both sides is expected to get improved. Beside simulation, the system is assembled and tested. Total power output is measured with ΔT from 5 to 30 K which increment ΔT is 5 K. 12.41 W of maximum power output at average temperature difference of 30 K is obtained when engine rate boosts to 3500 RPM. It is found that the open circuit voltage (V_{oc}) is increased linearly with ΔT and power output is increased rapidly with increasing the temperature difference. The V_{oc} and the P_{max} are expressed as a function of ΔT , which helps to forecast the system performance as $\Delta T > 30$ K.

For this system to harvest waste heat, the maximal power output is observed in the range of matched load of 23–30 Ω with increasing T_h from 323 to 403 K. This trend agrees with temperature dependent material property of electrical resistance. The efficiency of these 24 TEG modules is about 0.3% because of the insufficient Q_{in} in the TEG modules. One exception is the thermoelectric recovery of waste heat in which it is unnecessary to concern the cost of the thermal input. Other words, waste heats are considered as low-cost and even no-cost resources. Consequently, low conversion efficiency is not a serious issue that we have to take into account.

Future work is planned to conduct a liquid cooling system in place of this forced convection one. To concern the interior space design, energy conversion efficiency and system power capacity that would be very important for automobiles in next generation.

Acknowledgements

This research was funded by National Science Council, NSC 98-3114-E-007-008. Chung-Shan Institute of Science & Technology also supported this project and gave technological assistance.

References

- [1] Talom HL, Beyene A. Heat recovery from automotive engine. *Appl Therm Eng* 2009;29:439–44.
- [2] Ono K, Suzuki RO. Thermoelectric power generation: converting low-grade heat into electricity. *J Miner Met Mater Soc* 1998;50:12–31.
- [3] Rowe DM. Thermoelectrics, an environmentally-friendly source of electrical power. *Renew Energy* 1999;16:1251–6.
- [4] Haidar JG, Ghogel JL. Waste heat recovery from the exhaust of low-power diesel engine using thermal electric generators. In: *Proc int conf thermoelectrics*, Beijing, China, 2001. p. 413–7.
- [5] Yang J. Potential applications of thermoelectric waste heat recovery in the automotive industry. In: *Proc int conf thermoelectrics* Clemson, USA, 2005. p. 155–9.
- [6] Eisenhut C, Bitschi A. Thermoelectric conversion system based on geothermal and solar heat. In: *Proc int conf thermoelectrics*; 2006. p. 510–5.

- [7] LaGrandeur J, Crane D, Mazar S, Eder A. Automotive waste heat conversion to electric power using skutterudite, TAGS, PbTe and BiTe. In: Proc int conf thermoelectrics Vienna, Austria, 2006. p. 343–8.
- [8] Hasebe M, Kamikawa Y, Meiarashi S. Thermoelectric generators using solar thermal energy in heated road pavement. In: Proc int conf thermoelectrics; 2006. p. 697–700.
- [9] Ota T, Fujita K, Tokura S, Uematsu K. Development of thermoelectric power generation system for industrial furnaces. In: Proc int conf thermoelectrics; 2006. p. 354–7.
- [10] Kajikawa T, Onishi T. Development for advanced thermoelectric conversion system. In: Proc int conf thermoelectrics Jeju, Korea, 2007. p. 322–30.
- [11] Lertsatitthanakorn C. Electrical performance analysis and economic evaluation of combined biomass cook stove thermoelectric (BITE) generator. *Bioresource Technol* 2007;98:1670–4.
- [12] Qiu K, Hayden ACS. Development of a thermoelectric self-powered residential heating system. *J Power Sources* 2008;180:884–9.
- [13] Poudel B, Hao Q, Ma Y, Lan Y, Minnich A, Yu B, et al. High-thermoelectric performance of nanostructured bismuth antimony telluride bulk alloys. *Science* 2008;320:634–8.
- [14] Boukai AI, Bunimovich Y, Tahir-Kheli J, Yu J-K, Goddard Iii WA, Heath JR. Silicon nanowires as efficient thermoelectric materials. *Nature* 2008;451:168–71.
- [15] Hochbaum AI, Chen R, Delgado RD, Liang W, Garnett EC, Najarian M, et al. Enhanced thermoelectric performance of rough silicon nanowires. *Nature* 2008;451:163–7.
- [16] Kushch AS, Bass JC, Ghamaty S, Elsner NB. Thermoelectric development at Hi-Z technology. In: Proc int conf thermoelectrics, Beijing, China, 2001. p. 422–30.
- [17] Hsiao YY, Chang WC, Chen SL. A mathematic model of thermoelectric module with applications on waste heat recovery from automobile engine. *Energy* 2010;35:1447–54.
- [18] Thacher EF, Helenbrook BT, Karri MA, Richter CJ. Testing of an automobile exhaust thermoelectric generator in a light truck. *Proc Inst Mech Eng Part D J Automob Eng* 2007;221:95–107.
- [19] Niu X, Yu J, Wang S. Experimental study on low-temperature waste heat thermoelectric generator. *J Power Sources* 2009;188:621–6.
- [20] Gou X, Xiao H, Yang S. Modeling experimental study and optimization on low-temperature waste heat thermoelectric generator system. *Appl Energy* 2010;87:3131–6.
- [21] Yao Da-Jeng, Yeh Ke-Jyun, Hsu Cheng-Ting, Yu Ben-Mou, Lee JS. Efficient reuse of waste energy. In: *IEEE nanotechnology magazine*, vol. 3; 2009. p. 28–33.
- [22] Hsu CT, Yao DJ, Ye KJ, Yu BM. Renewable energy of waste heat recovery system for automobiles. *J Renew Sustain Energy* 2010;2.